K x-ray emission from solid neon and from neon implanted into metals

G. Deconninck,[1,2] A. Lefebvre,[1] F. Bodart,[1] and M. Dubus[3]
[1]*LARN, Facultés Universitaires Notre-Dame de la Paix, B-5000 Namur, Belgium*
[2]*Université Catholique de Louvain, B-1348 Louvain-La-Neuve, Belgium*
[3]*Centre d'Etudes Nucléaires de Grenoble, Grenoble, France*
(Received 27 December 1994; revised manuscript received 19 June 1995)

The emission of *K* x-rays following the irradiation of solid Ne at various pressures is investigated. A cryogenic target of solid Ne at vapor pressure is obtained by the condensation of Ne gas on an aluminum backing maintained at a temperature of 5.5 K. This target is irradiated with 2-MeV H^+ and $^4He^+$, and the evolution of the target is controlled by the detection of backscattered particles. X-ray emission following the ionization of Ne is also detected during irradiation. It is observed that the x-ray spectra do not significantly differ from the atomic spectrum recorded on Ne gas. Samples of metals implanted with Ne ions are irradiated with 4-keV electrons and *K* x-ray spectra from Ne are recorded. Important broadening effects are observed on the $K\alpha_{1,2}$ lines; the satellites from double ionization are less seriously affected. It is observed that the total width of the $K\alpha_{1,2}$ band is directly related to the shear modulus of the metal.

PACS number(s): 34.50.Dy

I. INTRODUCTION

Solids of inert gases have been extensively studied during the past few decades. The emission and absorption of radiation in the uv region have been the subject of many experimental and theoretical works. However, a number of questions remain open in the case of solid Ne, since experimental measurements are rare and difficult due to the low melting point (24.4 K) and the low-*Z* value of Ne.

K x-ray spectra from Ne gas have been carefully analyzed by Ågren *et al.* [1]. The $K\alpha_{1,2}$ diagram lines at 848.6 eV and the five satellites from double ionization have been identified and interpreted in the *LS*-coupling scheme.

The existence of a $2p$ band in solid Ne was revealed by electron density curves in photoelectron spectroscopy using synchrotron radiation; a total bandwidth of 1.3 eV was observed in solid Ne at vapor pressure [2]. The $2p$ valence band of solid Ne was calculated by various authors. A total width of 0.45 eV was obtained by Kunz and Mickish [3] and 0.65 eV by Euwema *et al.* [4].

Noble gases are essentially unsoluble in metals [5]. When introduced by implantation (accelerated ions) they tend to form stable precipitates as observed for Ar, Kr, and Xe [6–8]. In the case of Ne two interesting observations have been reported. Vom Felde *et al.* [9] found fluid Ne bubbles at high pressure in Ne-implanted Al using EELS (electron energy loss spectroscopy) and TEM measurements. Luukkainen, Keinonen, and Erola [10] measured high-pressure Ne in Ta (6.4 GPa) and in Mo (8.8 GPa) using Doppler-shift attenuation. At such high pressures, Ne should be solid [11].

Evans and Mazey [12] have summarized the previous results by a simple equation that relates the pressure to the shear modulus of the host metal. In this paper we study the spectrum of *K* x-ray emission lines of Ne, implanted into a collection of polycrystalline metals, paying special attention to the influence of the shear modulus on the spectrum shape.

II. EXPERIMENTAL TECHNIQUES

X-ray emission was observed by the ionization of Ne targets with electrons, protons, and ^4He ions. Atomic spectra were obtained by the irradiation of a Ne gas cell with 2.8-MeV $^4He^+$ from the LARN Van de Graaff generator and with 4-keV electrons from an electron gun (LEEIX technique); details of these techniques have been described in previous papers [13–15]. A flat crystal x-ray spectrometer (beryl crystal) was used for the analysis of the spectra. The response function of the spectrometer around 848 eV ($K\alpha_{1,2}$ transition energy) in Ne is given by

$$f(E)=\frac{[1-b(E-E_0)]}{\left((E-E_0)^2+\frac{\Gamma^2}{4}\right)}, \tag{1}$$

where $b=0.19$ eV^{-1} and $\Gamma=0.73$ eV. This function is used in the deconvolution procedure of the spectra [13,14].

Cryogenic targets of solid Ne at vapor pressure were produced by letting a jet of Ne gas impinge on an aluminum substrate, cooled at 5.5 K by circulation of liquid helium. The cryogenic target system was located at the center of a 50-cm-diam scattering chamber equipped with surface barrier particle detectors and a flat crystal x-ray spectrometer. A pressure of 10^{-7} Torr was maintained in this chamber, installed on the extension tube of the 2-MeV Van de Graaff generator at the CENG laboratory [16]. The Ne jet took 10 min to produce a thick target (2.9 mg cm^{-2}). The thickness is estimated by 2-MeV proton backscattering and the purity was measured by 2-MeV $^4He^+$ backscattering.

Different metal samples (polycrystalline) were implanted with energetic Ne^+ ions (50 keV), resulting in the production of a stable layer (Gaussian shape density) of Ne under the metal surface. The depth profile of the implantation was measured by ^4He backscattering, nuclear resonant $^{20}Ne(p,\gamma)$ reactions induced by protons [16], and simulated using the TRIM 91.14 computer program [17].

III. *K* X RAYS FROM NEON GAS AT LOW PRESSURE

The emission of *K* x rays from Ne gas irradiated with 2.8-MeV $^4He^+$ ions has already been described in previous

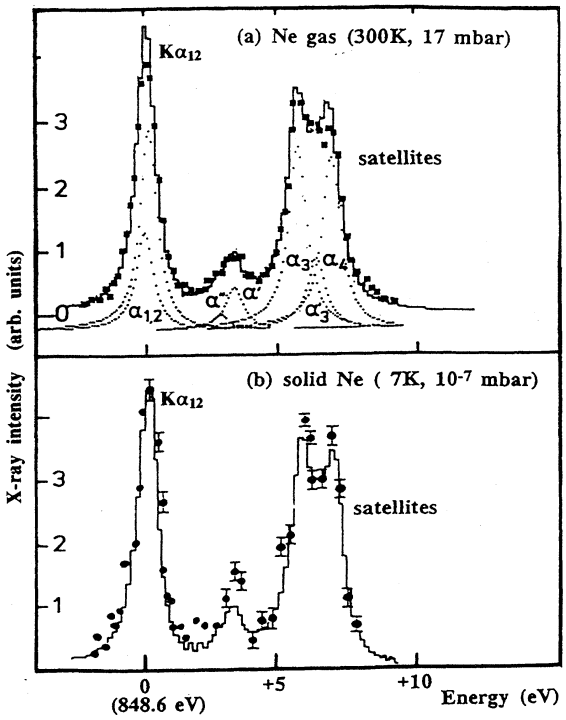

FIG. 1. K x-ray spectra from gas and solid Ne irradiated with ^{4}He particles. The spectra are obtained by diffraction on a beryl crystal and the angular scale has been converted into an energy scale. The zero-point energy corresponds to the $K\alpha_{1,2}$ transition at 848.6 eV. (a) Data from a Ne gas target (300 K, 17 mbar). (b) Data from a solid Ne target (7 K, 10^{-7} mbar). The different components ($K\alpha_{1,2}$, $K\alpha''$, $K\alpha'$, etc.) are represented by dotted lines; they have been calculated by convolution of the response function with the theoretical lines (the parameters of Ågren *et al.* [1]). The full line represents the sum of the different components. The dotted lines are shifted down for an easier reading.

papers [13,14]. The spectrum shows the atomic x-ray lines identified by Ågren *et al.*, i.e., a narrow $\alpha_{1,2}$ line that is an unresolved doublet from spin-orbit splitting (0.12 eV) and five satellites from double ionization ($\alpha'', \alpha', \alpha_3, \alpha_3', \alpha_4$). The relative intensity of the satellites depends on the ionization mode since multiple ionization results from two mechanisms: shake-off and Coulomb interactions. The spectrum is reproduced in Fig. 1(a); the solid line is the result of a calculation using the amplitudes given by Ågren *et al.* and the response function of the spectrometer [formula (1)]. Only one amplitude factor was introduced to match the satellite group intensity, which of course depends on the excitation mode. In the present paper, only the $K\alpha_{1,2}$ spectrum will be considered in the discussion; more data on the satellite shifts ΔE can be found in Ref. [15] and in Table I.

IV. X RAYS FROM CRYOGENIC SOLID NEON

The emission of K x rays from rare-gas solids has not, as far as we know, been reported before. The excitation of these x rays necessitates cryogenic systems to produce solid samples at vapor pressure. In the case of Ne, the spectrum consists of a doublet ($\alpha_{1,2}$) and a group of satellites from double ionization. The problem is to determine whether the existence of a $2p$ valence band [2] is reflected in the spectrum shape.

The cryogenic Ne target (melting point 24.4 K) was irradiated with a low-intensity beam (10 nA) of $^4He^+$ particles. X rays from ionization were detected by the flat crystal spectrograph and the particles scattered by the target were detected simultaneously. In such experimental conditions, the target temperature rises slowly during the irradiations and remains constant at 7 K during the measurements. The x-ray spectrum is reproduced in Fig. 1(b). When compared to the gas curve [Fig. 1(a)], it is found to be very similar to the atomic spectrum within the limits of the experimental resolution. The slight difference in the relative amplitude of the $\alpha'\alpha''$ satellites is attributed to the energy dependence of the cross section for double ionization. The statistics are rather poor in these experiments due to the low counting rate and to a rapid destruction of the target by sputtering. Better statistics were obtained when the sample was irradiated with 2-MeV protons. The K ionization cross section is higher and the target lifetime longer since erosion is proportional to the electronic stopping power [18], which is ten times smaller for protons than for ^{4}He ions at 2 MeV. Target thickness was controlled by the backscattering of protons during irradiation. We observed that the Ne ice target can tolerate a beam of 10 nA several hours without suffering appreciable deterioration. The spectrum of x rays detected during proton irradiation is reproduced in Fig. 2.

The K x-ray spectrum from 2-MeV protons on gas was recorded for comparison. Unfortunately, the presence of an overwhelming background completely ruins the spectrum. This background originates from γ rays produced by nuclear reactions on the collimators and in the gas cell. The comparison between x-ray spectra induced by protons on gas and solid Ne was impossible since there was no irradiation facilities in the scattering chamber. Fortunately, the main peak ($K\alpha_{12}$) is independent of the production mode. We have compared the electron-induced spectrum on gas to the proton-induced spectrum on solid Ne (Fig. 2). Once again, the solid spectrum shows a similarity to the gas spectrum in that there is no apparent broadening of the x-ray lines.

As mentioned above, the presence of a valence band with a total width of 1.3 eV was observed by Schwentzer *et al.* [2] in photoelectron measurements on a target of solid Ne obtained in similar conditions. The corresponding density of states (DOS) curve is reproduced in Fig. 2 (shaded line). In the same figure the x-ray spectrum calculated by convoluting the response function with the joint density of states for a transition from the supposed $2p$ valence band is reproduced (full line). A comparison with experimental data shows that a transition from the $2p$ valence band should significantly differ from the $K\alpha_{1,2}$ x-ray peak in gas. This is not the case in our experiments with ^{4}He and proton excitation.

We must point out here that the emission induced by protons originates from the whole irradiated volume. It corresponds to a depth of more than 10 μm below the surface. We know that sputtering originates from a depth of about 20 nm below the surface [18]. The effect of sputtering on the spectrum can therefore be considered negligible.

TABLE I. List of elements arranged by increasing values of the shear modulus μ. r and Δr are the depth and the width (FWHM) of the Ne implantation. D is the efficient depth for K shell ionization by 4-keV electrons. T_m is the melting temperature of the metal. P is the pressure sustained by Ne in the supposed solid inclusions. Γ_{tot} is the width (FWTM) of the $K\alpha_{12}$ distribution and ΔE is the satellite energy shift.

Metal	μ (GPa)	r (nm)	Δr (nm)	D (nm)	T_m (K)	P (GPa)	Γ_{tot} (eV)	ΔE (eV)
Pb [a]	5.7	58	77	49.6	600		0	0
Al	27.2	91	82	280.0	933		1.87	0.3
Au	28.2	37	50	29.8	1337		1.95	0.1
Ag	29.4	44	56	71.0	1235		1.62	0.2
Zr	36.8	63	73	123.4	2135		2.36	0.4
Nb	37.3	45	54	91.0	2641		2.44	0.3
Zn [a]	37.9	55	66	113.3	692		1.06	0.1
Ti	40.6	72	70	184.8	1933		2.36	0.3
Cu	46.4	44	52	95.5	1356		1.87	0.2
V	47.6	52	54	142.0	2163		2.60	0.4
Ta	70.0	40	56	36.9	3269		2.85	0.4
Co	76.3	41	47	92.5	1768	4.77 [b]	2.85	0.6
Fe	84.7	44	50	103.5	1808	5.29 [b]	2.77	0.4
Mo	122	44	54	76.3	2890	7.63 [b]	3.09	0.4
Be	150	105	62	297.0	1551	9.38 [b]	3.58	0.5
W	150	35	45	31.4	3683	9.44 [b]	3.66	0.5

[a]For Pb and Zn, the melting point is too low for the formation of overpressurized bubbles.
[b]The threshold for solidification of Ne at room temperature is 4.7 GPa.

From repeated measurements we conclude that x rays from solid Ne at vapor pressure are of a purely atomic nature. The expected broadening of the x-ray line due to the presence of a $2p$ valence band in the solid was not observed.

V. *K* X RAYS FROM NEON IMPLANTED INTO METALS

The ion implantation of atoms unsoluble in metals is an elegant way to produce small aggregates at room temperature. When implanted at the medium doses, low-energy ions

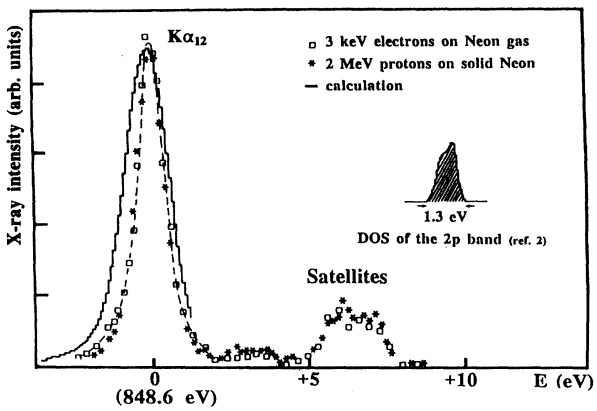

FIG. 2. K x-ray intensity curves from Ne (gas and solid) irradiated with protons and electrons. The squares represent the x-ray intensity from Ne gas irradiated with 3-keV electrons; the stars represent the results obtained on solid Ne (7 K) irradiated with a beam of 2-MeV protons. The full line is the result of a calculation for solid Ne postulating the existence of a 1.3-eV-wide valence band (shaded area) as observed in photoelectron experiments [2].

of Ar, Kr, and Xe gather in orientated solid aggregates [6–8] often called "bubbles." TEM studies indicate that the size of these bubbles is of the order of 1–5 nm [12]. Clustering is so dense that the implanted aggregates may become solid at room temperature, with the internal pressure ranging between 1 and 10 GPa. Such great pressures are mainly conditioned by the metal shear modulus μ for small concentrations (1–5 at. %) and by the surface tension γ for large radius bubbles produced at high concentrations. Using experimental results on Kr and Xe, Evans and Mazey [12] gave an empirical formula relating the internal pressure P to the shear metal modulus for small diameter inclusions:

$$P=\mu/\alpha\ , \tag{2}$$

where $\alpha=16\pm4$ and P and μ are in GPa. In Table I we have reproduced the known shear modulus for a collection of polycrystalline metals and the corresponding pressures estimated by formula (2).

In the case of Ne, measurements are rare; only one estimation was made by Luukkainen, Keinonen, and Erola [10]. Using the Doppler-shift attenuation technique, the pressures found for Ne in tantalum (6.4 GPa) and molybdenum (8.8 GPa) are in agreement with the estimations reproduced in Table I. Vom Felde *et al.* [9] reported the observation of fluid Ne bubbles in implanted aluminum. Ne is present in a fluid state since the pressure (1.7 GPa) is well below the threshold for solid Ne at room temperature [11].

The diffraction of x rays from Ne contained in small diamond cells at high pressure and room temperature was extensively studied by Finger *et al.* using the diamond anvil technique [11]; they obtained a (P,V) diagram for Ne between 4.75 and 14.42 GPa. In this pressure range Ne is solid at room temperature. They found that solid Ne is a highly

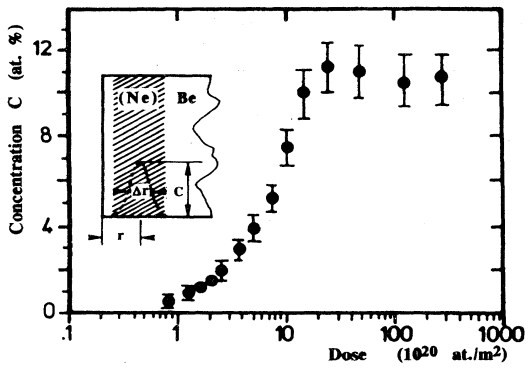

FIG. 3. Concentration in at. % (at the maximum of the implantation distribution) versus the implanted dose in Be. The concentration is measured by the backscattering of $^4He^+$ ions.

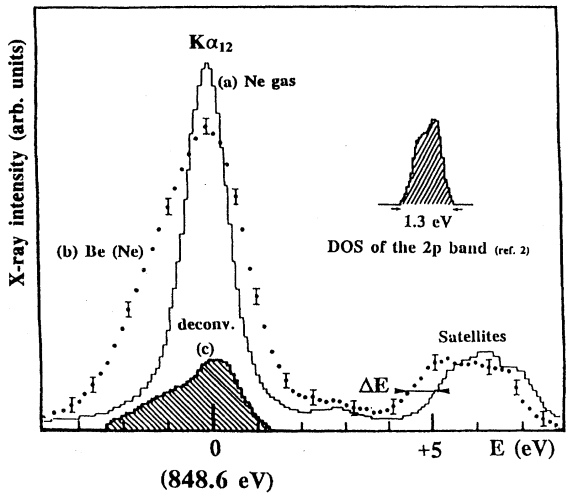

FIG. 4. Comparison between x-ray spectra from Ne gas and from Ne implanted into beryllium. (a) X-ray intensity curve from Ne gas irradiated with electrons (reproduced from Fig. 2). (b) X-ray intensity curve from Ne in Be irradiated with electrons. When compared with curve (a) a considerable broadening of the $K\alpha_{1,2}$ component is observed. The satellite group is shifted to lower energy by $\Delta E = 0.5$ eV. (c) X-ray spectrum obtained by deconvolution of curve (b) ($K\alpha_{1,2}$ component only). This curve represents the DOS of the $2p$ band. The DOS observed on solid Ne at vapor pressure (7 K) is reproduced for comparison (EPS data [2]).

compressible solid, adapting its structure to the changing shape of the diamond cell. The structure is fcc close packed with a lattice parameter of 4.38 Å at vapor pressure decreasing to 3.78 Å at 4.8 GPa and 3.47 Å at 14.4 GPa (at room temperature). These enormous variations of the atomic parameters should normally be reflected in the band structure and in the x-ray spectra.

When Ne is implanted into a metal at room temperature, it remains clustered in a stable, Gaussian-like distribution well below the surface of the sample (see the inset in Fig. 3). The parameters of the distribution are the mean range r (average depth in nanometers) and full width at half maximum Δr (in nanometers), which are obtained by ^4He backscattering in the case of Be and Al [15]. For higher-Z metals the nuclear resonant reaction $^{20}Ne(p,\gamma)$ [16] or the TRIM program [17] is used. These parameters are shown in Table I for a series of host metals.

The samples are irradiated with electrons. The implantation depth is not critical since the Ne layer always lies in the high-efficiency region for x-ray emission (efficient depth). This efficient depth D for K-shell ionization by 4-keV electrons is calculated by [19]

$$D = 25\frac{A}{\rho Z^{n/2}}(E_0^n - E_x^n), \tag{3}$$

where D is in nanometers; $n = 1.2\ (1-0.29\log_{10}Z)^{-1}$; E_0 is the electron energy in keV; E_x is the ionization energy of the K shell; and A, Z, and ρ are, respectively, the atomic weight, the atomic number, and the metal density (g cm^{-3}). The efficient depth D for 4-keV electrons in various metals is reported in Table I.

X rays from implanted Ne can only be analyzed if there are no interfering x rays from the host metal in the 830–880 eV energy range. To check for the absence of x-ray lines, we have irradiated all the metals reported in Table I before implantation.

Beryllium is a good candidate since the density of the implantation is easily measured by backscattering. For this reason a number of measurements have been performed on this metal. An example is given in Fig. 3, where the concentration of Ne in at. % (measured at the maximum of the Gaussian density) is plotted versus the implanted dose (in at. %/m^2). Saturation was observed at 11 at. %.

The spectrum of x rays detected during the electron irradiation of a beryllium sample implanted with 5×10^{20} Ne at./m^2 is shown in Fig. 4 [curve (b)] and the spectrum from a gas target is also shown for comparison [curve (a)]. Considerable differences can be observed between the two spectra. The narrow $K\alpha_{1,2}$ peak observed becomes a broad distribution and the satellites are all shifted to lower energy ($\Delta E = 0.5$ eV). After unfolding for the experimental response and for the Lorentzian distribution of the 1-s^{-1} initial state ($\Gamma = 0.24$ eV), the $K\alpha_{1,2}$ radiation spectrum shows an asymmetric distribution [curve (c)], which is the actual x-ray spectrum emitted by Ne trapped in the metal. The width [full width at tenth maximum (FWTM)] of the distribution is 3.6 eV. If this wide distribution is due to a band structure, then curve (c) is the DOS for the $K\alpha_{1,2}$ transition. The DOS from solid Ne at vapor pressure is shown for comparison (shaded inset in Fig. 4). The asymmetric shape was explained by a spin-orbit splitting of 0.5 eV [2]. A similar interpretation of the DOS curve [Fig. 4(c)] would give a magnitude of 1 eV for the spin-orbit splitting. The total width of the DOS (FWTM) is 3.6 eV and the position of the maximum coincides with the atomic line at 848.6 eV. The satellite curve has also been deconvoluted, yielding five single lines. This group remains practically unmodified; only a small shift of 0.5 eV was observed (Fig. 4).

Similar measurements have been performed on a collection of different metals implanted with

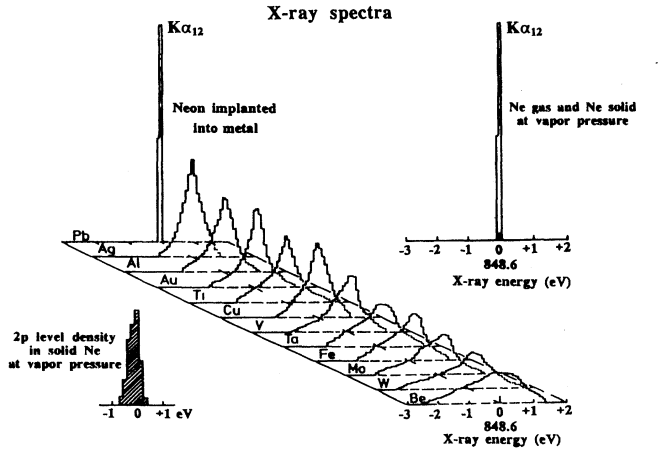

FIG. 5. $K\alpha_{1,2}$ x-ray spectra obtained by deconvolution from Ne implanted into different metals. The narrow lines observed in Ne gas and in solid Ne are also represented. The $2p$ density of states from solid Ne at vapor pressure is shown for comparison (shaded curve).

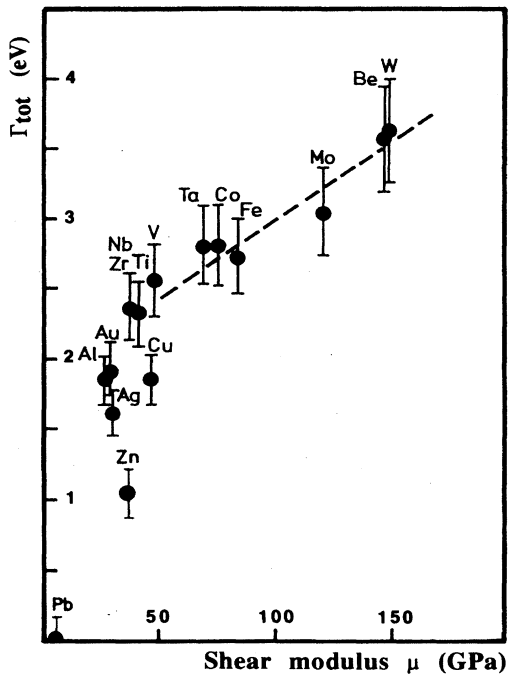

FIG. 6. Total width of the $K\alpha_{1,2}$ distribution plotted versus the shear modulus of the different host metals. The dashed lines represents the linear approximation [formula (3)].

Ne (Pb, Al, Au, Ag, Zr, Nb, Zn, Ti, Cu, V, Ta, Co, Fe, Mo, Be, W). The spectra were found to be very similar to the Be spectrum, except that the width of the $K\alpha_{1,2}$ band strongly depends on the host metal. All the parameters relevant to our problem can be found in Table I. This table has been constructed according to increasing shear modulus values. The error on the determination Γ_{tot} was principally due to the high-energy tail of the $K\alpha_{1,2}$ component superimposed on the weak α' and α'' satellites. This error was minimized by taking the FWTM as a definition of the total width Γ_{tot}; the error was estimated at 10%.

The $K\alpha_{1,2}$ bands obtained by deconvolution of the $K\alpha_{1,2}$ spectra observed on the different metals are shown in Fig. 5, where a panoramic view of the $2p$ density of states is presented. These curves are presented according to decreasing shear modulus values. A wide distribution was observed in Be and W; the width decreases gradually to a narrow line when Ne is imbedded in low shear modulus metals. A similar relation was observed when Γ_{tot} was plotted versus other metal parameters: surface energy, volume compression coefficient, and Young modulus [15]. Our presentation (versus shear modulus) corresponds to the model used by Evans and Mazey for inert gases implanted into metals [12].

The total width Γ_{tot} gradually decreases from 3.6 eV in Be (9.38 GPa) to 1.6 eV in Ag (1.84 GPa). The Pb spectrum is a narrow line corresponding exactly to the $2p$ atomic doublet at 848.6 eV (Table I).

In Fig. 6 we have plotted Γ_{tot} versus the shear modulus μ for different metals; an evident correlation is observed between these two parameters. By simple linear regression (broken line in Fig. 6) we obtain the following relation, which is valid for $\Gamma_{tot}>2$ eV:

$$\Gamma_{tot}=0.012\mu+1.72, \quad (4)$$

where Γ_{tot} is in eV and μ is in GPa. The satellite structure is not seriously modified except for a small shift ranging between 0.1 and 0.5 eV, depending on the metal. The magnitude of the shift is reported in Table I and the error is estimated at 30%.

VI. DOSE DEPENDENCE OF THE WIDTH Γ_{tot}

The width Γ_{tot} was measured in Be for different implanted doses. Between each dose determination, the sample was irradiated with electrons and x rays were detected. In Fig. 7 we

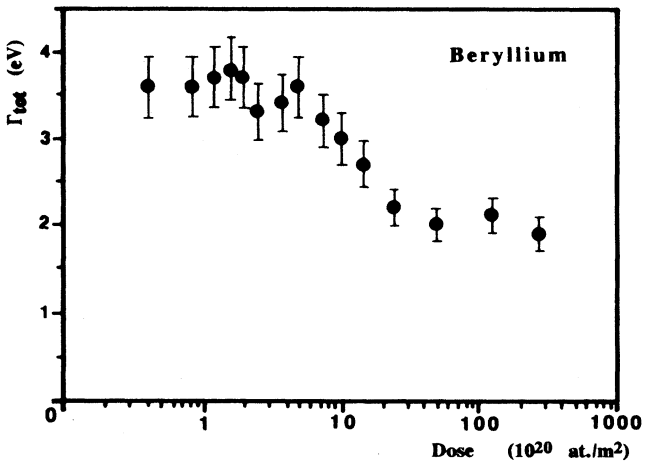

FIG. 7. Dose dependence of the width Γ_{tot} for a sample of implanted Be.

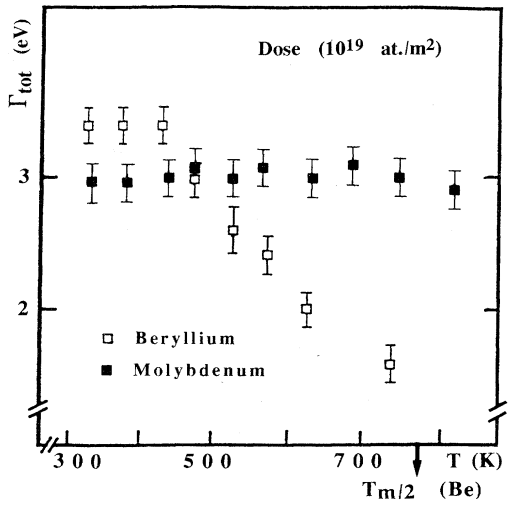

FIG. 8. Temperature dependence of the width Γ_{tot} of Be and Mo implanted with Ne. Each measurement is made after heating for 60 min at the corresponding temperature.

present the observed width Γ_{tot} versus the implanted dose. Within experimental error, Γ_{tot} remains constant up to 5×10^{20} at./m^2 and then decreases with increasing doses and remains constant for doses higher than 4×10^{21} at./m^2.

VII. TEMPERATURE DEPENDENCE OF Γ_{tot}

Measurements on different metals were undertaken to investigate the temperature dependence of the width Γ_{tot}. Samples of Ne-implanted metals were heated in vacuum and kept at a constant temperature T for 60 min and then irradiated with electrons to obtain the width Γ_{tot} of the $K\alpha$ x-ray spectrum. In Fig. 8 we report the results obtained on Be and on Mo; the width Γ_{tot} is plotted versus the heating temperature. In the case of Be we observe that the width remains constant (3–4 eV) up to 400 K and then slowly decreases. For Mo the total width Γ_{tot} remains constant in the observed temperature range (up to 700 K).

VIII. CONCLUSIONS

In this paper we essentially report original observations on the emission of K x rays from Ne. We first investigated solid Ne at vapor pressure (7 K) and found that the $K\alpha_{1,2}$ spectrum is a narrow line, typical of atomic Ne, a surprising result since we know that a $2p$ valence band ($\Gamma_{tot}=1.3$ eV) was observed [2] in solid Ne photoelectron spectra in similar experimental conditions.

It is well known that there is an abundant production of atomic and molecular excitons (Ne*, Ne_2^*, and Ne_2^+) in the irradiated volume [18]. In x-ray spectroscopy any excitation or ionization of the outer electron shell with a simultaneous ionization of the K shell (necessary to produce a K x ray) should result in a relative increase of the satellite amplitude. Such an effect was not observed in our experiments.

An important broadening of the $K\alpha_{12}$ x-ray line is observed in Ne-implanted metals. We know that the implantation is stable in time and also under moderate thermal treatment. Like Vom Felde *et al.* [9] and Luukkainen, Keinonen, and Erola [10], we now make the hypothesis that Ne (like Ar, Kr, and Xe) is present in fluid bubbles or solid inclusions in the host metal. Under this hypothesis and supposing that formula (2) is valid for Ne, we can interpret Fig. 5 as a relation between the pressure P in the inclusions and the width Γ_{tot}.

At a pressure of 4.83 GPa, Ne must be solid. From formula (2) this corresponds to a shear modulus between 58 and 96 GPa. For higher values Ne is solid. In this case, the following elements would have solid inclusions: Ta,Co,Fe,Mo,Be,W.

Various reasons can be found to account for the broadening of x-ray lines. Let us mention (a) the important contraction of the Ne crystal dimensions under pressure, (b) the interaction of the atoms of the bubble surface with the conduction electrons of the host metal, and (c) the excitation of phonons. The most straightforward hypothesis is that the contraction is due to the pressure, resulting in a reduction of the lattice dimensions. A reduction of the lattice parameters should normally induce a broadening of the valence-band width Γ_{tot} [20]. According to the results of Ref. [11], the lattice parameter of solid Ne under a pressure of 9.38 GPa is 3.58 Å. This high pressure corresponds to the case of Be. When compared to 4.38 Å, which is the lattice parameter of solid Ne at vapor pressure, the reduction is to the order of 17%, a factor that can qualitatively explain the huge broadening of the $K\alpha_{1,2}$ band [3,4].

Another hypothesis is the interaction of the electrons from the $2p$ band with the conduction electrons of the metal (phonon interactions), which, however, does not explain the absence of broadening of the satellite lines. We could also postulate that the broadening is simply due to the superposition of narrow peaks at different energies originating from bubbles at various pressures. In this hypothesis, however, the spectrum shape should be affected by thermal treatment or by changing the density of the bubbles. Such effects have not been observed in experiments conducted in our laboratory.

If we accept the hypothesis of solid Ne inclusions in high shear modulus metals (Ta,Co,Fe,Mo,Be,W), from formula (2) and (4) Γ_{tot} becomes a measure of the pressure sustained by Ne in these inclusions. All other elements (Pb,Zn,Al,Au,Ag,Zr,Nb,Ti,Cu) have a low shear modulus value. For all these elements Ne should exist in fluid bubble.

The dose dependence of the width (Fig. 7) now becomes easy to understand. It is known that with increasing doses of rare gas, there is nucleation, growth of the bubbles, and above a given dose, the pressure decreases. We observed that Γ_{tot} has the same behavior as the pressure.

The temperature behavior of Γ_{tot} (Fig. 8) can also be explained. In the case of Be, the width decreases above 400 K and around half melting-point temperature $T_{m/2}$ (775 K), the width is considerably reduced. In the case of Mo ($T_{m/2}=1445$ K) the width remains constant up to 800 K. It is known that $T_{m/2}$ corresponds to the thermal generation of mobile vacancies, which can migrate to the inclusion and partly release the excess pressure. Our results are in accor-

dance with this statement if we postulate that the width is proportional to the pressure.

We have tried to confirm our results on metals by photoelectron spectroscopy using an SSX 100 spectrometer equipped with an argon gun for surface erosion. This surface technique did not show the presence of Ne implanted into beryllium, probably because of sputtering, which produces the liberation of the Ne gas during the erosion process.

More measurements are needed (TEM) to confirm the existence of solid inclusions in high shear modulus metals. If this hypothesis is confirmed, x-ray emission will probably remain one of the sole techniques yielding information on the valence-band density of states of Ne implanted in metals. More measurements on monocrystalline metals are in progress, attempting to confirm the results and the direct TEM observation of presumed Ne inclusions.

ACKNOWLEDGMENTS

We wish to thank Professor J. J. Pireaux for the photoelectron measurements at LISE Laboratory in Namur, Professor A. A. Lucas for helpful discussions, and the FRFC (Belgium) for financial support of this project. We are also indebted to the DRS.G/SBT/LACC at the CENG center in Grenoble (France) for their help in cryogenic facilities and the realization of solid Ne samples.

[1] M. Ågren, J. Nordgren, L. Selander, C. Nordling, and K. Siegbahn, J. Electron Spectrosc. Relat. Phenom. **14**, 27 (1978).
[2] N. Schwentzer, F. J. Himpsel, V. Saile, M. Skibowski, W. Steinmann, and E. E. Koch, Phys. Rev. Lett. **34**, 528 (1975).
[3] A. Barry Kunz and D. J. Mickish, Phys. Rev. B **8**, 779 (1973).
[4] R. N. Euwema, G. G. Wepfer, G. T. Surratt, and D. L. Wilhite, Phys. Rev. B **9**, 5249 (1974).
[5] A. A. Lucas, Physica B&C **127B**, 225 (1984).
[6] J. H. Evans and D. J. Mazey, J. Phys. F **15**, L1 (1985).
[7] C. Templier, H. Garen, J. Grilhé, and J. Delafond, C. R. Acad. Sci. Paris **300**, 543 (1985).
[8] J. C. Desoyer, C. Templier, J. Delafond, and H. Garem, Nucl. Instrum. Methods Phys. Res. Sect. B **19/20**, 450 (1987).
[9] A. Vom Felde, J. Fink, Th. Müller-Heinzerling, J. Pflüger, B. Scheerer, G. Linker, and D. Kaletta, Phys. Rev. Lett. **53**, 922 (1984).
[10] A. Luukkainen, J. Keinonen, and M. Erola, Phys. Rev. B **32**, 4814 (1985).
[11] L. W. Finger, R. M. Hazen, G. Zou, H. K. Mao, and P. M. Bell, Appl. Phys. Lett. **39**, 892 (1981).
[12] J. H. Evans and D. J. Mazey, J. Nucl. Mater. **138**, 176 (1986).
[13] A. Lefebvre and G. Deconninck, Nucl. Instrum. Methods Phys. Res. Sect. B **15**, 616 (1986).
[14] G. Deconninck and A. Lefebvre, Mater. Sci. Eng. **90**, 167 (1987).
[15] A. Lefebvre, Thèse de Doctorat, LARN, Facultés Universitaires de Namur, 1990 (unpublished).
[16] A. Banse-Lefebvre, G. Deconninck, and G. Terwagne, Nucl. Instrum. Methods Phys. Res. Sect. B **66**, 205 (1992).
[17] J. F. Ziegler, J. P. Biersack, and Y. Littmark, *TRIM 91.14, The Stopping Power and Range of Ions in Solids* (Pergamon, New York, 1985).
[18] O. Ellegaard, J. Schou, and H. Sorensen, Nucl. Instrum. Methods Phys. Res. Sect. B **13**, 567 (1986).
[19] A. Roche, M. Charbonnier, F. Gaillard, M. Romand, and R. Bador, Appl. Surf. Sci. **9**, 227 (1981).
[20] E. Boursey, J. Y. Roncin, and H. Damany, Phys. Rev. Lett. **3**, 1279 (1970).